Naval Research Laboratory

Washington, DC 20375-5320

NRL/MR/6384--96-7907

Shock and Damage in Marine Composite Structures

C.T. DYKA

Geo-Centers, Inc.
10903 Indian Head Highway
Fort Washington, MD

R.R. INGEL

Mechanics and Materials Branch
Materials Science and Technology Division

December 31, 1996

REPORT DOCUMENTATION PAGE

Form Approved OMB No. 0704-0188

1. AGENCY USE ONLY *(Leave Blank)*	2. REPORT DATE	3. REPORT TYPE AND DATES COVERED
	December 31, 1996	Final

4. TITLE AND SUBTITLE

Shock and Damage in Marine Composite Structures

5. FUNDING NUMBERS

6. AUTHOR(S)

C.T. Dyka* and R.R. Ingel

7. PERFORMING ORGANIZATION NAME(S) AND ADDRESS(ES)

Naval Research Laboratory
Washington, DC 20375-5320

8. PERFORMING ORGANIZATION REPORT NUMBER

NRL/MR/6384--96-7907

9. SPONSORING/MONITORING AGENCY NAME(S) AND ADDRESS(ES)

ARPA
Arlington, VA 22209

10. SPONSORING/MONITORING AGENCY REPORT NUMBER

11. SUPPLEMENTARY NOTES

*Geo-Centers, Inc., 10903 Indian Head Highway, Fort Washington, MD 20744

12a. DISTRIBUTION/AVAILABILITY STATEMENT

Approved for public release distribution unlimited.

12b. DISTRIBUTION CODE

13. ABSTRACT *(Maximum 200 words)*

This report is a summary of our recent efforts here at NRL in developing a methodology for predicting the response of thick composite materials subjected to multi-dimensional shock loadings. A focus of this work has been the development of a 1D, 2D, and 3D evolving damage theory applicable to highly transient loading environments such as underwater shock and impact. This approach is phenomenological in nature and has achieved a degree of success. Comparisons to 2D composite plates impact experiments have been very encouraging. In this work, we assume a local material damage and effective resiting area perspective, in which the evolving damage is considered to be a vector quantity. The 1D theory includes explicit dispersion/viscoelastic effects as well.

14. SUBJECT TERMS

Composites	Damage mechanics	Plates & Shells	Undex
Finite element	Explicit analysis	Transient	
Shock	Impact	Wave propagation	

15. NUMBER OF PAGES

46

16. PRICE CODE

17. SECURITY CLASSIFICATION OF REPORT	18. SECURITY CLASSIFICATION OF THIS PAGE	19. SECURITY CLASSIFICATION OF ABSTRACT	20. LIMITATION OF ABSTRACT
UNCLASSIFIED	UNCLASSIFIED	UNCLASSIFIED	UL

NSN 7540-01-280-5500

Standard Form 298 (Rev. 2-89)
Prescribed by ANSI Std 239-18
298-102

CONTENTS

SHOCK AND DAMAGE IN MARINE COMPOSITE STRUCTURES

1.0 INTRODUCTION

The use of composite structures for present and future naval applications represents an important development. Composites offer significant advantages over the traditional metals due to their strength, stiffness and lightweight characteristics. However, the behavior of these composite structures, particularly under highly transient shock loadings, is not well understood at the present time. Material and structural failure models, subjected to dynamic loading environments are not currently well developed especially for thick, polymer matrix, fiber reinforced, composite materials. Also, the experimental data base for these materials in naval type structures is very sparse. References [1-3] are indicative of some of the experimental work that has been performed on composite structures subjected to underwater shock environments.

Composite structures represent a radical departure from the traditional ductile, homogeneous, isotropic metal structures. Under severe loadings, metals deform plasticity due to slip along shear lines. Current analysis methods, which are rooted in continuum mechanics, have been developed and applied based upon traditional metal type of structures where failures usually have been more global in nature due to the metal ductility. The use of high strength metals in naval structures has lead to more brittle types of problems, such as weld cracks. But modern finite element techniques and plasticity constitutive models can still be widely applied due to the homogeneous and nearly isotropic nature of the metals.

Fiber reinforced polymer composites are very heterogeneous materials that combine high performance fibers in a viscoelastic matrix. There are several levels of heterogeneities to consider: between layers, between the fiber and matrix, and also heterogeneities in the form of voids arising from processing the composite. Thus composites are more difficult to characterize and model with the standard "deterministic", continuum mechanics based, finite element programs currently available.

In addition, composite structures tend to be highly dispersive to propagating waves, and deform nonlinearly under severe load due to the development of networks of micro-cracks. Because of all these features, the shock response and the development of damage in composites is not a well understood phenomena.

Manuscript approved October 30, 1996.

Continuum damage mechanics, see for instance [4-14], is in general a developing field of research that is not yet mature. Damage theories have progressed further for metal structures due to their more homogeneous, isotropic and ductile nature. The abilitiy to model and predict localization and shear banding as well as the propagation of large cracks has certainly progressed in recent years. Plasticity assumptions which allow the use of the scalar variables, such as effective stress and strain, are responsible for much of this success in metal structures.

Much of the modern concept of damage mechanics is based upon the idea of area reduction. Kachanov [15] in 1958 first purposed a phenomenological theory of creep damage by introducing a scalar damage variable D to characterize the material degradation. Later Rabotnov [16] interpreted D as representing the fraction of damaged material. The effective resisting area of the local material degrades initially from A to $\overline{A}$ due to damage where:

$$\overline{A} = (1 - D)A \tag{1.1}$$

In one dimension (1D), the effective stress is defined as:

$$\overline{\sigma} = \sigma / (1 - D) \tag{1.2}$$

This concept of local material damage and effective resisting area has been extended to include vector and higher order tensor definitions of damage more applicable to orthotropic and anisotropic material. The literature in continuum damage is quite extensive, see for instance [4-11] and [24-26] for more of a discussion regarding metals and plasticity, and [12-14] for discussion of brittle and composite materials.

Although such concepts as local damage described by D, which may be represented as a scaler, vector or higher order tensor, are quite useful one must always remember that composites are a very heterogeneous media in general. Continuum based models are therefore particularily difficult to apply given the statistical nature of the media. The linking between scales, micro-meso-macro (structural) is also extremely important but at present not well understood. Issues associated with homogenization (see for instance [17]) must be adequately addressed. Because of these factors, much of what has been and is being developed in the continuum damage field is limited to specific materials and structures and relatively narrow in application. Phenomenological approaches have been prevalent.

One very important exception to this restriction is the dissipated energy approach developed by

Mast et al in [18]. In this work, the authors couple the calculation of the damage in a test specimen directly to the computation of the dissipated energy. An assumption is made that the material behaves as indicated in Figure 1.1, where where the stress strain curve follows path ABC for loading and by path CA for unloading. The area between curves ABC and CA represents the dissipated energy of the material. Using the experimental data, a dissipated energy density function φ is obtained for the composite material via interpolation. The stress $\underline{\sigma}$ is postulated to be a function of strain and a single state variable ξ or:

$$\underline{\sigma} = \underline{\underline{C}}(\xi, \varepsilon) \tag{1.3}$$

where $\underline{\underline{C}}$ is the constitutive tensor. Next the work potential:

$$\Psi(\underline{\varepsilon}) = \Phi(\underline{\varepsilon}) + \varphi(\underline{\varepsilon}) \tag{1.4}$$

where $\Phi(\underline{\varepsilon})$ is equal to the energy density recovered if the material were to unload linearly from its present state. The constitutive tensor is then determined from:

$$\underline{\sigma} = \underline{\nabla}_{\underline{\varepsilon}} \Psi(\xi, \varepsilon) \tag{1.5}$$

The analytical and experimental approach in [18] is limited to static or quasi-static conditions, can not detect through thickness delaminations, and defines damage only in a scalar sense. Thus, directional damage can not be differentiated. However, it has been highly successful and is a very important contribution to the field of damage mechanics because it directly couples a series of experiments and loading conditions for composite materials to the calculation of the constitutive tensor and damage. This work has the added advantage that unlike other approaches, it does not require the estimation of several additional parameters that are good only for a narrow range of material properties.

In general in this report, we shall emphasize the evolving damage approach and results developed in [19-22]. In section 2, 1D and 2D continuum damage models are reviewed and compared to the experimental results [23] obtained from impact tests on thick composite circular plates. In section 3, 1D parametric studies of graphite/peek plates subjected to underwater shock (UNDEX) are discussed. Approximate ranges for incipient damage and extensive damage are indicated for the weight of the charge and its standout distance.

In section 4, the 3D continuum damage theory developed in [22] is summarized. A preliminary version of the 3D damage model has been programmed into the commercial finite element

program ABAQUS/EXPLICIT but not yet tested. In general as discussed in section 4 and [22], the modeling of evolving 3D damage in composite plates and shells represents an extremely difficult task to do efficiently and accurately. Several hurdles remain to overcome before robust 3D capabilities will be available for general use.

Finally in section 5, a summary and some conclusions are given, from the perspective of work done here at NRL, regarding the state of the art of modeling the shock response and damage in composites.

1.1 Through thickness modeling and damage

As we have seen, composite structures differ significantly from metal structures in their response to loading environments. Composite plates and shells are typically thicker than comparable metal structures. Couple this with the lower compliances of their matrix components, and fiber reinforced composites typically display much more transverse shear effects in general. Current finite element codes can account only in a crude fashion for transverse shear effects.

Fiber reinforced composites are also more heterogeneous and anisotropic than typical structural metals. The layering of various ply combinations produces a complex arrangement that can only be approximate in an average sense. Without some sort of homogenization procedure, one is forced to attempt a detailed modeling throught the thickness direction of the plate or shell structure using solid elements. This is typically completely unfeasible given the thickness to length ratios of typical plate/shell structures, which would require large number of solid elements.

Through thickness (or delamination) damage, especially in dynamic loading environments, is much more of a concern in composite structures than it is in metal structures. This type of damage is also very difficult to accurately model. The standard displacement finite element codes that are popular today do not contain plate or shell elements which can account for through thickness (normal direction) deformation and stress even in a crude fashion. These types of plate/shell elements simply do not exist.

To account for through thickness effects using the currently available commercial finite element

method (FEM) technology one has no other choice but to use solid elements - thus producing very large models to solve. In sections 2, 3 and 4, more will be said about modeling through the thickness.

1.2 Dynamic Versus Static Behavior

Composite structures, especially laminated plates and shells, comprise a very heterogeneous media, whose dynamic response can be exceedingly complex. If the wavelength of the loading and the response of the material is very long compared to the scale of the inhomogeneity, then the material response is governed by effective properties of the equivalent homogenized media. However, if the composite structure is subjected to shock environments, then the wavelengths of the loading and response of the structure will be much shorter. In this case, the characteristic dimensions of the heterogeneous media become much more important. The interfaces between the material phase cause wave reflection and refraction. The energy is thus spread or "dispersed' over many wavelengths.

Dispersion can also be present in composite materials due to the viscoelastic nature of the matrix. Viscoelasticity represents a history dependent nonlinear response that is difficult to include even approximately in numerical models. The response of viscoelastic material is also usually frequency dependent. Couple this to the general anisotropic and heterogeneous nature of a laminated structure, and the inclusion of viscoelasticity effects into numerical models becomes even more difficult to accurately account for.

In [21], Nemes and Randles discuss the inclusion of viscoelasticity into a 1D damage model. They obtain an excellent fit to experimental data [23] for the impact of a flyer plates on axisymmetric graphite/peek composite plates. Again this work is 1D, in the through thickness direction.

Viscoelasticity and material damping remain a significant problem to overcome for numerical models of even linear composite structures. Current finite element modeling approaches appear to use various forms of structural damping such as Rayleigh to try to account for the damping caused by the viscoelasticity. For models that include evolving damage, other than [21,22] explicit viscoelasticity effects have been largely ignored.

With respect to metal structures, Nemes et al. in a series of papers [24-26] developed a modified form of the viscoplastic damage constitutive theory of Perzyna [27] and applied it to model high strain rate behavior occuring in plate impact spall fracture. Although they were quite successful and obtained excellent correlation to experimental data, this type of approach, which is phenomenological based, requires extensive experimental data to even estimate the several material and rate parameters that are needed. The range of applicability of this viscoplastic damage approach is somewhat narrow, and of course restricted to metals.

In a dynamic loading situation, damage to the structure evolves in a very short period of time . Many of the thermodynamically based approaches are simply not completely valid because the structure is not in equilibrium. Damage occurs very quickly.

As mentioned in section 1.1, through thickness or delamination damage for a composite structure is an important consideration especially for a dynamic load such as impact or UNDEX. Composites are much more susceptible to this type of damage because they are very heterogeneous, are ususally thicker, have a fairly low modulus for the matrix, and a lower wave speed (especially throught the thickness) than comparable metal structures. For instance under an impact loading to a plate or shell structure, the compression wave passes through the thickness and is reflected off the backface as a tension wave. If the unloading or release wave, which is also tensile, meets this reflected wave delamination can occur in a composite if the tensile strength of the matrix is exceeded. Because the composite is typically thicker and has a lower wave speed than its metal counterpart, the release wave has more time and distance to meet the reflected wave and set up this situation for the composite.

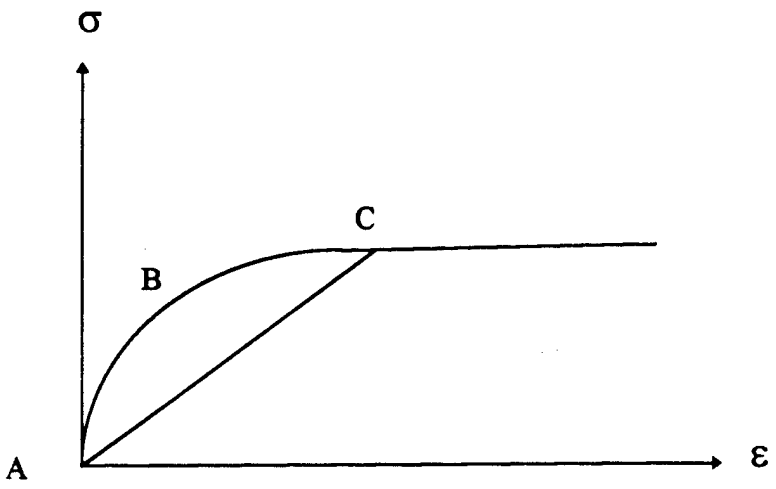

Figure 1.1 Assumed material behavior

2. 1D AND 2D CONTINUUM DAMAGE

In this section, we first summarize the NRL 2D continuum damage model (CDM) developed in [19,20]. This is followed by a comparison of 1D and 2D models to available experimental data [23] in subsections 2.2 and 2.3.

2.1 Summary of the NRL 2D Continuum Damage Model

References [19,20] develop a 2D continuum damage model (CDM) that employs an evolving vector damage theory for transversely isotropic materials. This theory is intended for application to highly transient loading situations such as impact and underwater shock. Figure 2.1 indicates a typical laminated composite. An assumption of transverse isotropy is made. The matrix damage is characterized by a vector or [14]:

$$\underline{\overline{V}} = V_1 \underline{e}_1 + V_2 \underline{e}_2 + V_3 \underline{e}_3 \tag{2.1}$$

where $\underline{e}_i$ i=1,2,3 are the unit normals along the material coordinate directions shown in Figure 2.1. In this phenomenological treatment, the damage magnitude is interpreted simply in terms of a fractional reduction in certain of the elastic properties. The V_1 component represents a network of matrix cracks in the 2-3 plane which induce delaminations throught the thickness direction of the laminate. The V_2 and V_3 components of damage are caused by matrix cracks which may traverse or lie between the reinforcing fibers, but do not break the fibers. Since a transverse isotropic assumption is made, the inplane components of the damage vector V_2 and V_3 are combined into the scalar V_S by:

$$V_S = (V_2^2 + V_3^2)^{1/2} \tag{2.2}$$

Thus, the inplane damage V_S is characterized by a scalar with a general direction that is perpendicular to the V_1 damage.

The evolving damage components V_1 and V_S vary from 0 (undamaged) to 1 (complete failure at the material point). The damage components are assumed by Nemes and Randles [19,20] to reduce the elastic properties of the composite at the material point in the transversely isotropic media as follows:

$$
\begin{aligned}
E_{11} &= (1 - V_l^2)E_{11}^0 \\
E_{22} &= (1 - \alpha_1 V_S^2)E_{22}^0 \\
G_{12} &= (1 - V_l^2)(1 - \alpha_2 V_S^2)G_{12}^0 \\
\nu_{12} &= (1 - V_l^2)(1 - \alpha_3 V_S^2)\nu_{12}^0 \\
\nu_{23} &= (1 - \alpha_4 V_S^2)\nu_{23}^0
\end{aligned}
\tag{2.3}
$$

where E, G, and ν denote the directional elastic moduli, shear moduli and Poisson's ratios. The superscript "0" denotes virgin properties and the fractions $0<\alpha_i<1$, i=1 - 4 are included to prevent a complete loss of material integrity as $V_S \rightarrow 1$.

Damage evolution and rate dependency is introduced in the 2D Nemes and Randles CDM approach by assuming a dependency on the current state of damage, some stress above a current threshold, and material properties controlling damage evolution rates. Both V_l and V_S types of damage are assumed to be governed by a scalar threshold function F (analogous to a yield function in plasticity) of the form:

$$
\begin{aligned}
F(\underline{\sigma}, \bar{f}(\underline{V})) &\leq 0 \quad \text{for no growth and} \\
&> 0 \quad \text{for damage growth}
\end{aligned}
\tag{2.4}
$$

where $\underline{\sigma}$ is the current stress tensor, $\bar{f}$ is an array of current threshold parameters which is a function of $\underline{V}$, the current damage vector.

The threshold function F is assumed by Nemes and Randles to be similar in form to the Mohr-Coulomb [28] type of yield criteria used in plasticity. This allows the strength of the material to be dependent on the tension. The form of F is assumed to be:

$$
F(\underline{\sigma}, \bar{f}) = (1 + (\tau / f_3)^{1/2} - (f_1 - \sigma) / f_2 \tag{2.5}
$$

In (2.5), τ and σ represent effective types of shear and tension stresses and differ in form for V_l or V_S type of damage evolution. The parameters f_i I=1,2,3 are related to specific growth threshold strengths (σ_G and τ_G) and the Coulomb friction tangent φ_{G12} as:

$$
\begin{aligned}
\sigma_{G1} &= f_1 - f_2 \text{ (tension threshold)} \\
\tau_{G1} &= f_3 \cdot ((f_1 / f_2)^2 - 1)^{1/2} \text{ (shear threshold)} \\
\varphi_{G1} &= f_3 / f_2
\end{aligned}
\tag{2.6}
$$

For the V_1 component of the damage, σ and τ in (2.5) are assumed to be of the form:

$$\sigma = \sigma_{11} \quad \text{(tension only)}$$

$$\tau = \sigma_{12} \tag{2.7}$$

The growth threshold strengths and Coulomb friction tangent in (2.6) are then postulated to depend on the V_1 damage as:

$$\sigma_{G1} = (1 - V_1^2)\sigma_{G10}$$

$$\tau_{G1} = (1 - V_1^2)\tau_{G10} \tag{2.8}$$

$$\varphi_{G1} = \varphi_{G10} + V_1^2(\varphi_{G11} - \varphi_{G10})$$

where the "0" subscript denotes virgin ($V_1 = 0$) threshold properties. Equations (2.8) are substituted into (2.6) and solved for f_1, f_2 and f_3. A similar approach is used to determine f_i for i=1,2,3 for V_S damage - see [19].

The evolution for V_1 and V_S damage completes the CDM constitutive description. The rate forms for V_1 and V_S damage used are:

$$\frac{dV_1}{dt} = (d_1 / \sigma_{G10})^{n_1} / (\eta_1(1 - V_1^2) \tag{2.9a}$$

$$\frac{dV_S}{dt} = (d_S / \sigma_{GS0})^{n_S} / \eta_S \tag{2.9b}$$

where n_1, η_1 and n_S, η_S are empircally based material constants, while d_1 and d_S represent distances from the threshold (yield) surfaces for V_1 and V_S damage. Thus, if d_1 or d_2 is zero, the rate of the damage growth will also be zero. Note in (2.9a) as $V_1 \to 1$, an acceleration to a castastrophic failure occurs, while in (2.9b) no explicit dependence on V_S is assumed for dV_S / dt.

Overall, the 2D CDM approach developed by Nemes and Randles [19-20] is very appealing and has had some success. However, like all phenomenological theories, it requires several material parameters that can only be estimated through pertinent experiments on specific laminated composites. In addition, this appproach like so many others does not adequately address the explicit viscoelastic nature of the matrix in the plane of the fibers. In [21,22], viscoelasticity is

added to a 1D version of the CDM, and good agreement is obtained with the experimental data for the impacted composite plates [23]. Sections 2.2 and 2.3 contain further discussion.

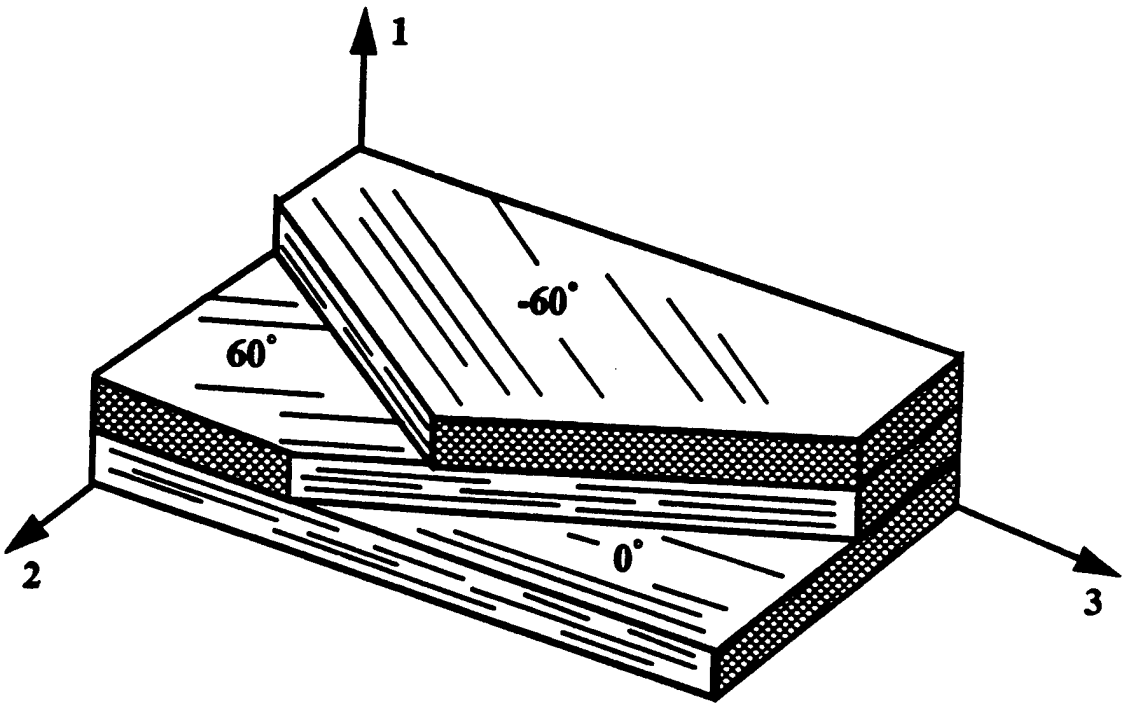

Figure 2.1.1 Typical laminated composite.

2.2 COMPARISONS OF 1D MODELS TO EXPERIMENTAL RESULTS

Impact experiments were conducted on axisymmetric graphite/peek and graphite/epoxy plates for the U.S. Naval Research Lab on the Phillips Lab Impact Facility 102 mm gas gun, using standard plate-impact techniques. Two types of flyer-plate impact experiments were conducted - see [23]. The first were transmitted wave tests, while the second set of experiments were spallation tests. The flyer consisted of axisymmetric polymethylmethacrylate (PMMA) plates.

One dimensional (1D) numerical simulations, using the WONDY [29] finite difference computer program, for these sets of experiments are reported in [21] and [22]. the inclusion of viscoelasticity effects in the through thickness direction produced 1D numerical results that compared very well to the experimental test data. In these detailed computer models, hundreds of difference points or zones were used to model through the thickness of the flyer and plate in order to accurately describe the shock structure. Figure 2.2.1 is taken from [21] and it compares the computed and measured particle velocities of the backface of the plates in the spall experiments (referred to as shots). In general, the comparison is very good. In Figure 2.2.2, again from [21], computed V_1 damage profiles through the plates are indicated for various experiments (shots). A value near 1.0 indicates total failure at that material point. These predictions compare reasonably well to observed damage (see [23]) and ultrasonic examination [21].

1D numerical simulations with the NRL 2D CDM have also been investigated using the finite element codes PRONTO2D and more recently ABAQUS/EXPLICIT - see [22]. In these 2D models of 1D behavior, explicit viscoelasticity has not been included through the thickness, and the models are much coarser than the very refined WONDY models. Even so, these results compare quite well in general to the WONDY runs and experimental data.

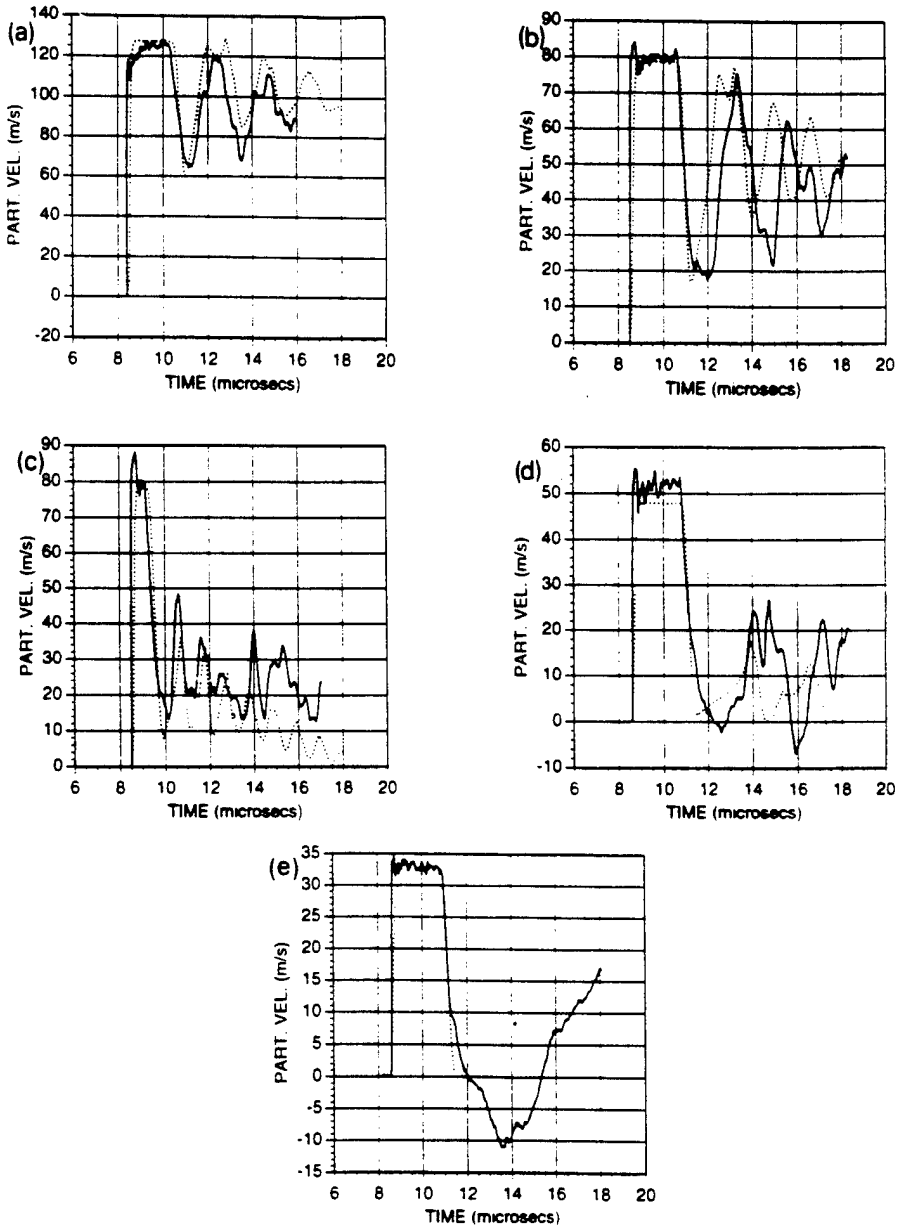

Figure 2.2.1 Comparison of computed and measured particle velocity in spall experiments (····· computed, _____ experiment): (a) shot 3360; (b) shot 3357; (c) shot 3362; (d) shot 3358; (e) shot 3368.

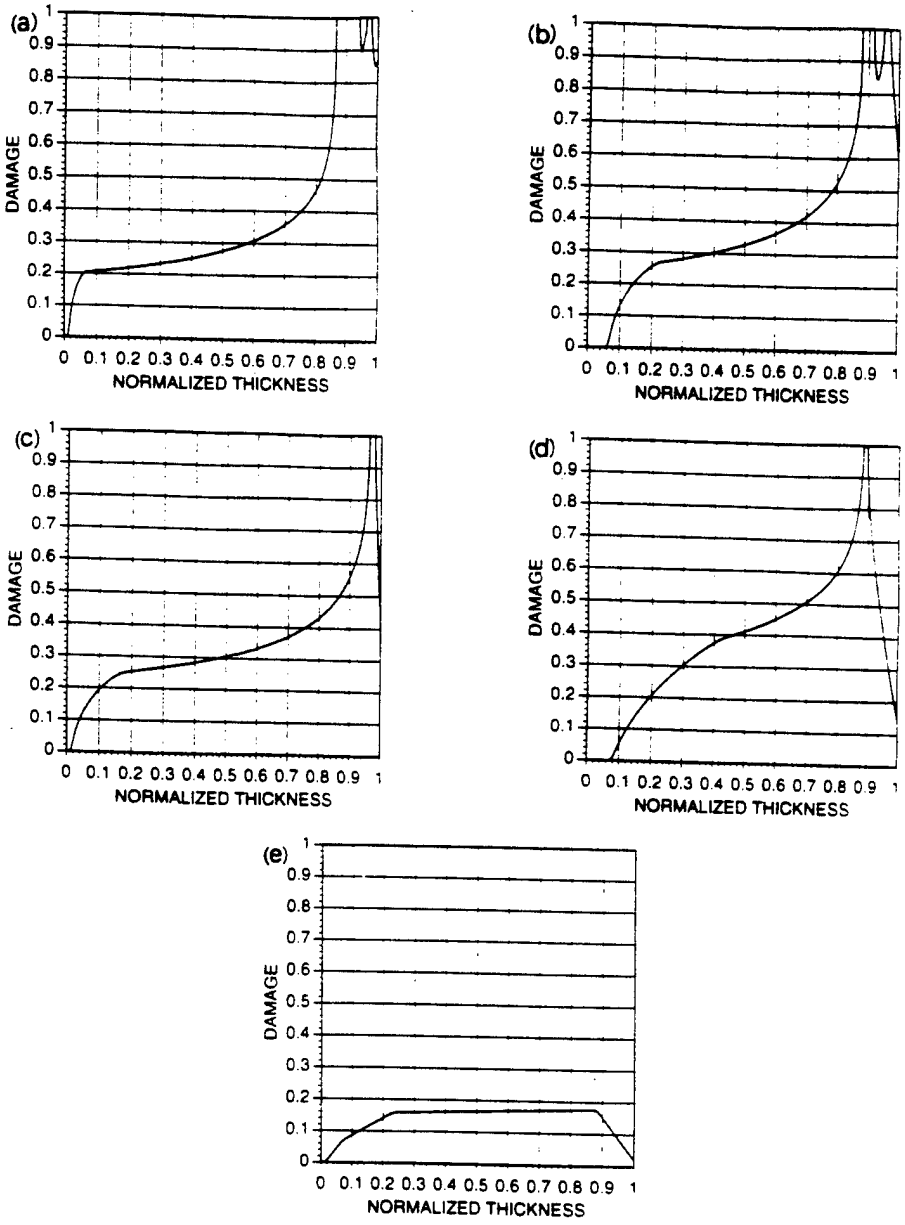

Figure 2.2.2 Computed damage profile through the specimen thickness (normalized): (a)shot 3360; (b) shot 3357; (c) shot 3362; (d) shot 3358; (e) shot 3368.

2.3 COMPARISONS OF 2D MODELS TO EXPERIMENTAL IMPACT RESULTS

Coarse 2D finite element models, using the PRONTO2D program, were constructed in [22] and compared well to the experimental impact tests in [23]. As indicated in section 2.2, the 2D NRL continuum damage model (described in section 2.1) has also been implemented into the explicit finite element code ABAQUS/EXPLICIT, and currently is available on the NRL Cray-EL.

Before discussing specific models, some comments concerning the modeling of 2D and of course 3D structures are in order. In our 1D simulations, hundreds of finite differnce points (WONDY analysis) or finite elements (PRONTO2D analysis) were employed through the plate thickness to accurately capture the propagation of the shock wave and the insuing damage. For 2D analysis this would translate into hundreds of elements through the thickness. Due to aspect ratio considerations, this level of refinement would require tens of thousands of elements to model just a 2D plate and flyer - which is completely impractical. In addition, 2D analyses require much longer times than 1D runs due to flexural and shear waves that develop in the plates.

Thus in our limited number of 2D models we have analyzed here at NRL, our purpose has not been to accurately capture the propagation and structure of the shock wave, along with the flexural and shear waves. But rather we have limited ourselves, due primarily to computer costs, to coarser models in which to predict overall damage patterns in the plates and estimates of peak backface velocities.

Figure 2.3.1 indicates a 2000 element axisymmetric model of a PMMA flyer and a graphite/peek plate using ABAQUS/EXPLICIT. A 30x50 grid of 2D, 4 node elements were used for the plate - 30 elements through the thickness. A grid of 10x50 elements was employed to discretize the flyer. In the 2D simulations, which were run on the NRL Cray-EL, the flyer was given an initial velocity of 93 m/sec, which corresponds to shot 3357 in the 1D runs in Figures 2.2.1 and 2.2.2, and the experimental test [23].

In Figure 2.3.2, the predicted backface velocity of the plate is indicated. Although the shape of this curves does not compare that well to Figure 2.2.1b, this coarse 2D model does predict a maximum particle velocity of approximately 77 m/sec, which is very close to both the refined WONDY prediction and the measured velocity. Figure 2.3.3 described the predicted through thickness V1 damage along the centerline of the axisymmetric graphite/peek plate for the 2000

element ABAQUS/EXPLICIT model. This result compares reasonably well to Figure 2.2.2b and the refined WONDY model.

In general, we are encouraged by these results from coarse 2D models with the NRL 2D continuum damage theory. Applications to other composite plates as well as parametric studies can be done with this capability, which has been programmed as a user written subroutine for ABAQUS/EXPLICIT.

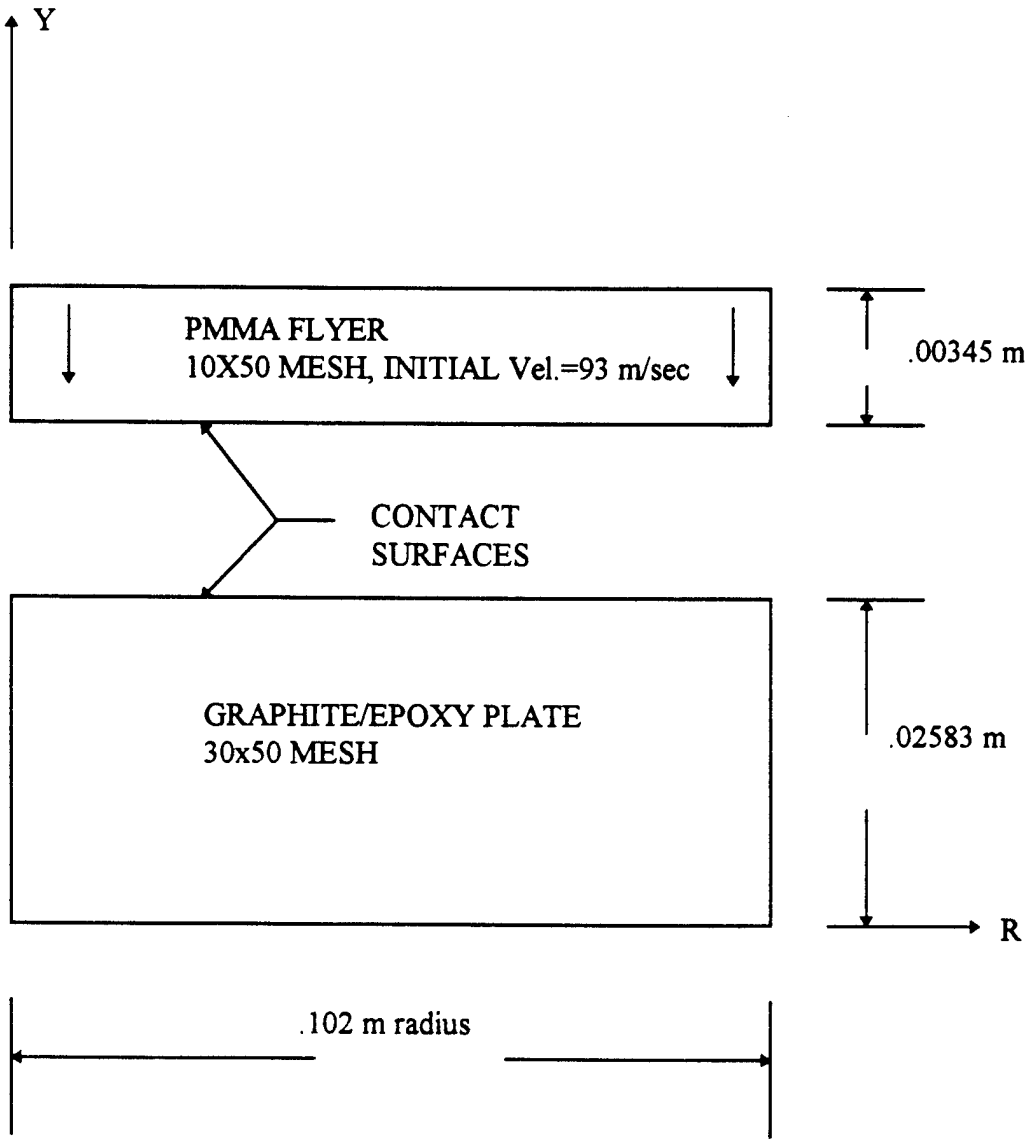

Figure 2.3.1 2000 element axisymmetric model of a PMMA flyer impacting a graphite/epoxy plate.

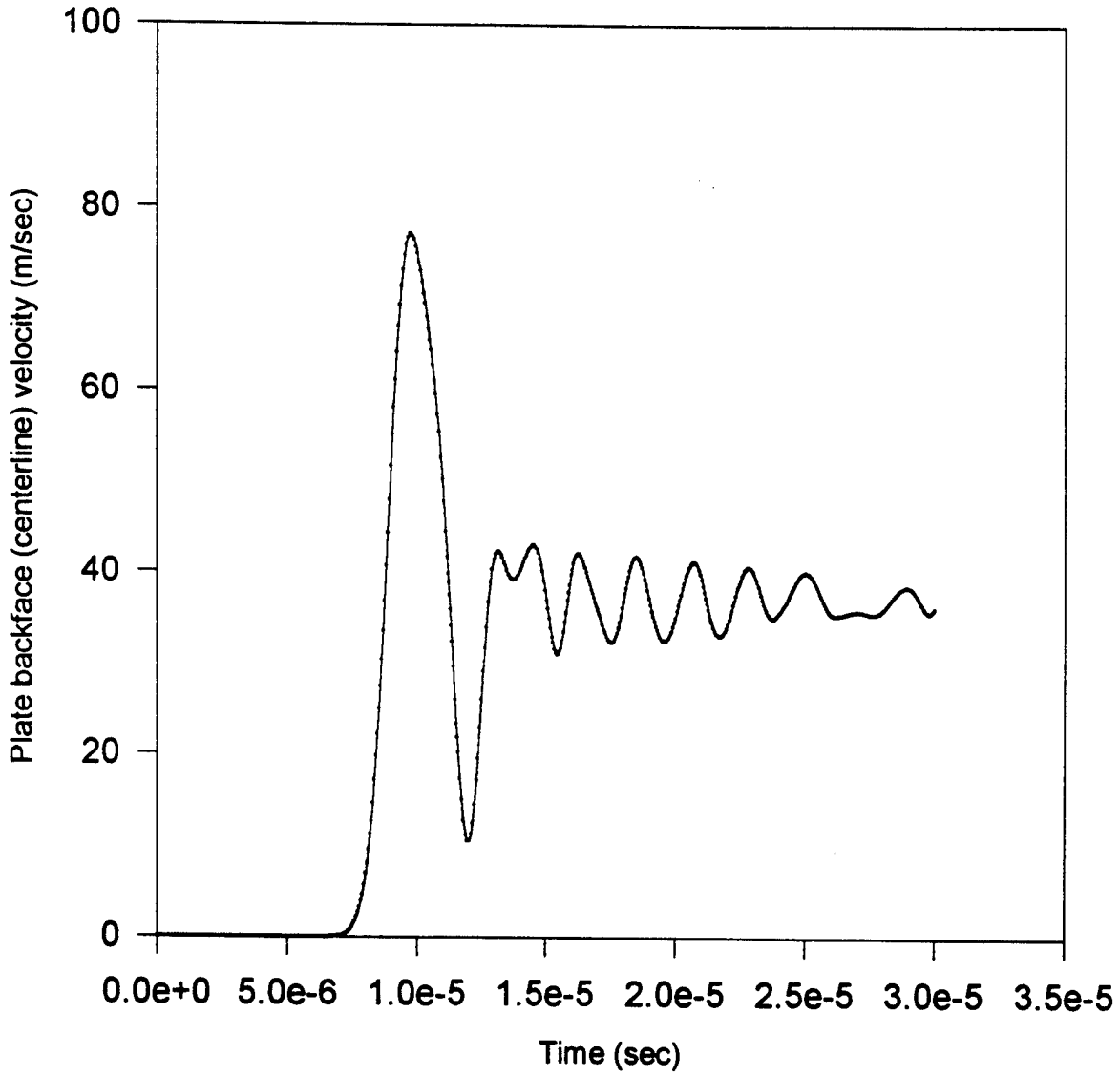

Figure 2.3.2 Centerline backface velocity of the plate for the 2000 element model.

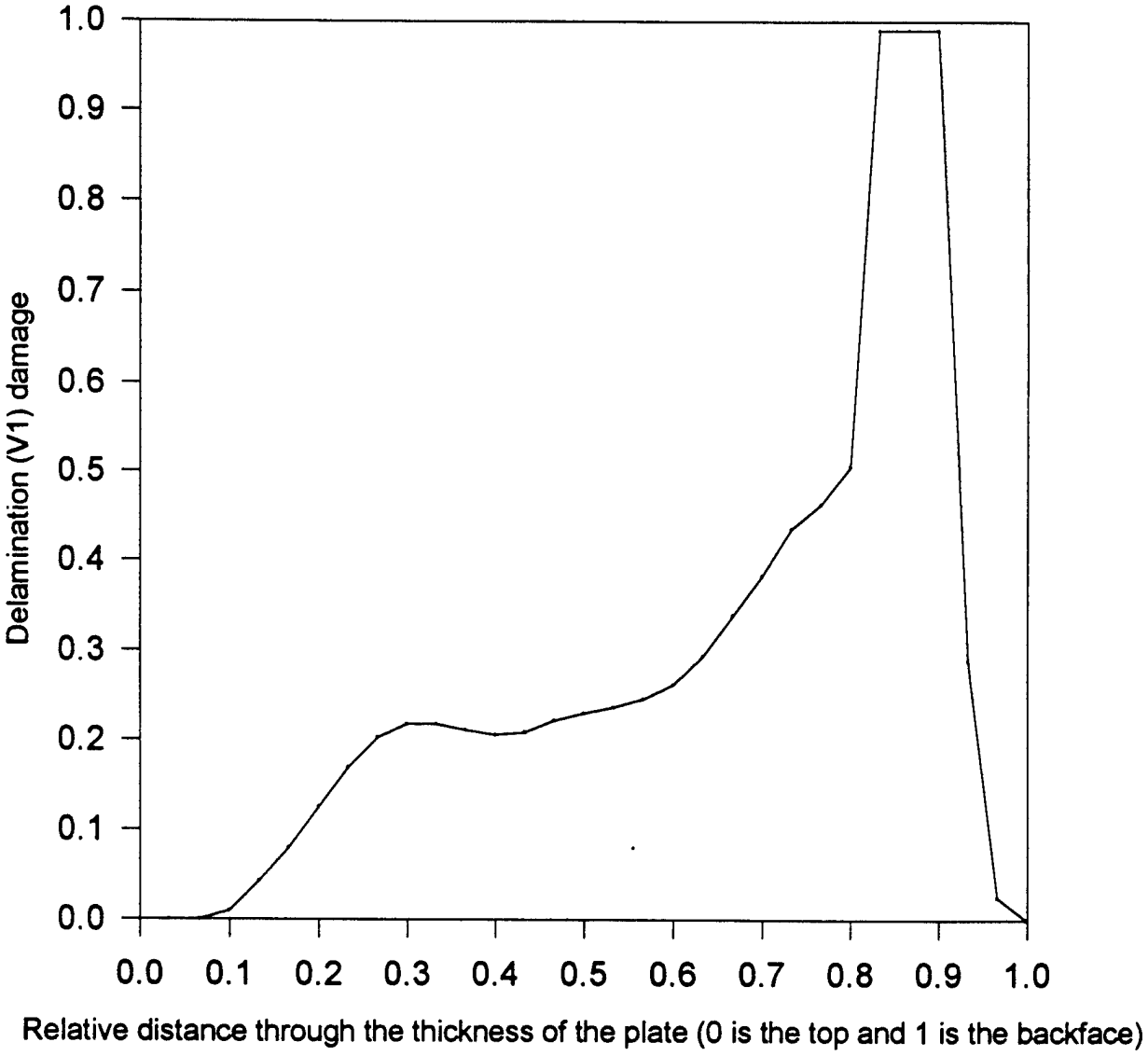

Figure 2.3.3 Delamination (V1) damage through the centerline of the plate for the 2000 element model.

3. FLUID-STRUCTURE INTERACTION MODELS

In this section 1D results from the modeling of graphite/peek plates subjected to underwater shock are examined. The evolving damage model developed by Nemes and Randles [19,20] has been employed.

3.1 1D Models

In [22], a 1D version of the 2D evolving damage model of Nemes and Randles was extended to include dispersion effects. A series of simulations were performed with the WONDY [29] finite difference computer program to predict the response of composite graphite/peek plates from 2 to 8 inches thick. The plates were subjected to simulated near field underwater explosions. The intent of these analyses, which are documented in [22], was to assess the extent of spallation damage for various charge weights and ranges, and to determine the approximate boundaries of incipient and complete spallation. The history of a TNT explosive pulse passing through a fixed spatial point can be expressed as [30]:

$$p = p_0 e^{-t/\theta} \tag{3.1}$$

where p_0 is the initial pressure and θ the exponential decay constant. Using Aaron's law p_0 and θ can be expressed as:

$$p_0 = 0.519\left(\frac{W^{1/3}}{R}\right)^{1.13} \tag{3.2}$$

$$\theta = 0.925 \times 10^{-4}$$

in which p_0 is given in kilobars, θ in seconds, R is the range in meters (m), and W is the charge mass in kilograms (kg). The value of W in (3.2) for this study ranged from 5 kg to 30 kg, with R varying from .5 to 1.5 m.

For seawater, the following material properties (SI units) were employed in the modeling:

$$\rho_w = 1000 \quad kg/m^3 \tag{3.3}$$

$$c_w = 1500 \quad m/s$$

$$s_w = 1.75$$

where ρ_w is the density and c_w is the water speed. The variable s_w comes from a linear shock velocity u_s to particle velocity u_p relationship of the form:

$$u_s = c_w + s_w \cdot u_p \tag{3.4}$$

The material constants used for the graphite/peek plates were:

bulk properties

$$\rho = 1579 \ \ kg/m^3 \tag{3.5a}$$

$c_0 = 3000$ m / s (wave speed through the thickness)

$E_{11} = 13.45 \times 10^9$ Pa (through thickness modulus)

$E_{22} = 69.0 \times 10^9$ Pa (inplane modulus)

$\nu_{12} = 0.04$ (transverse) and $\nu_{13} = 0.3$ (inplane)

damage parameters (see section 2.1 and [22])

$$\eta_1 = 1.0 \times 10^{-6}, \ \ n_1 = 1.0, \ \ \sigma_{G0} = 70 \times 10^6 \text{ Pa} \tag{3.5b}$$

and the dispersion parameters (see [22])

$$\lambda_1 = 0, \ \ \lambda_2 = 5.0 \times 10^{-6}, \ \ \gamma_1 = 0, \ \ \gamma_2 = 0.81 \tag{3.5c}$$

In Figure 3.1, a WONDY model for the composite plate and fluid media is indicated. For these 1D analyses, a very fine finite difference grid (zones) was employed to capture the damage and to accurately model the shock wave as it moved throught the fluid and into the plate. For full 2D (and especially 3D problems), which are discussed in section 3.2, a much coarser grid must obviously be employed, otherwise the models would become far too large to efficiently analyze. Also, we note in Figure 3.1 that only 1 inch of the fluid was included in the model, and no silent or non-reflecting boundary conditions were required at point A. In this model, our concern was strictly with the damage that would occur once the compressive wave moves through the fluid into the plate and is reflected at the free end B as a tensile wave. The analysis was terminated before any spurious reflections from A could reach the plate.

Figures 3.2a,b and c summarize the WONDY damage predictions for 2, 4 and 8 inch thick graphite/peek plates. The estimated boundaries of incipient and complete spallation are indicated in these three plots in which range and weight of charge have been varied. We note that in these WONDY analyses dispersion/viscoelastic effects have been included along with the 1D damage models (see [22]). Including dispersion/viscoelastic material behavior tends to slightly mitigate the overall damage predictions due to the material damping that is introduced in the structural model.

Next we will apply the 2D transversely isotropic continuum damage theory [19-20], which has been programmed into ABAQUS/EXPLICIT to the 1D fluid-structure problem indicated in Figure 3.1. (See section 2.1 for a discussion of the 2D damage theory, and [22] for the remaining values of the various elastic variables and damage parameters used for the graphite/peek plate). The 2D damage theory does not explicitly contain viscoelastic capabilities that can account for all the damping that is present in these types of composite structures. Figure 3.3 describes the 2D model for this 1D problem. Note that for this 2D model, a pseudo infinite element and several buffer fluid elements were employed to prevent any reflections from the top of the fluid model. In general, this was not necessary since the analysis was terminated before any reflections from the top of the fluid could reach the plate. A total of 156 2D elements were used - 55 in the fluid and 100 through the plate. The FEM model is thus relatively coarse compared to the very fine WONDY model indicated in Figure 3.1, but it will still be sufficient. Figure 3.4 indicates the through thickness damage profile predictions from the ABAQUS/EXPLICIT model for a 2 inch thick graphite/peek plate subjected to a charge of 10 kg at a range of one meter. In general, some damage is indicated near the top of the plate in Figure 3.4, but there is no spallation. This results compares reasonably well to the through thickness damage results from a refined WONDY analysis (not shown).

Overall, the WONDY and ABAQUS/EXPLICIT models that were run indicate that based on 1D models the charges need to be very close in to do significant delamination damage to the composite graphite/peek plates considered.

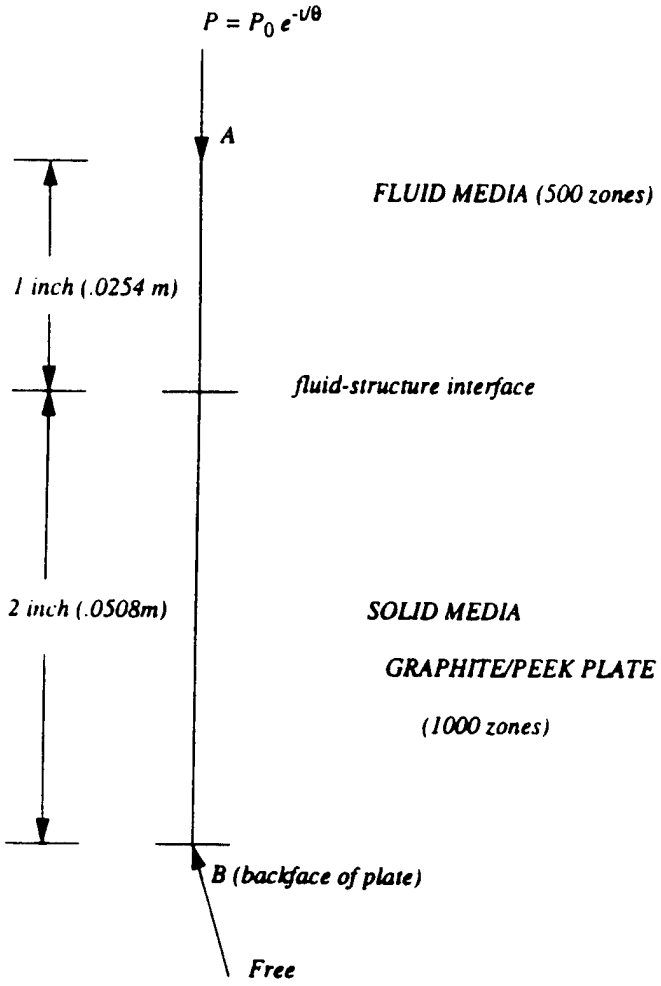

Figure 3.1 WONDY model for a graphite/peek plate subjected to underwater shock (1D analysis).

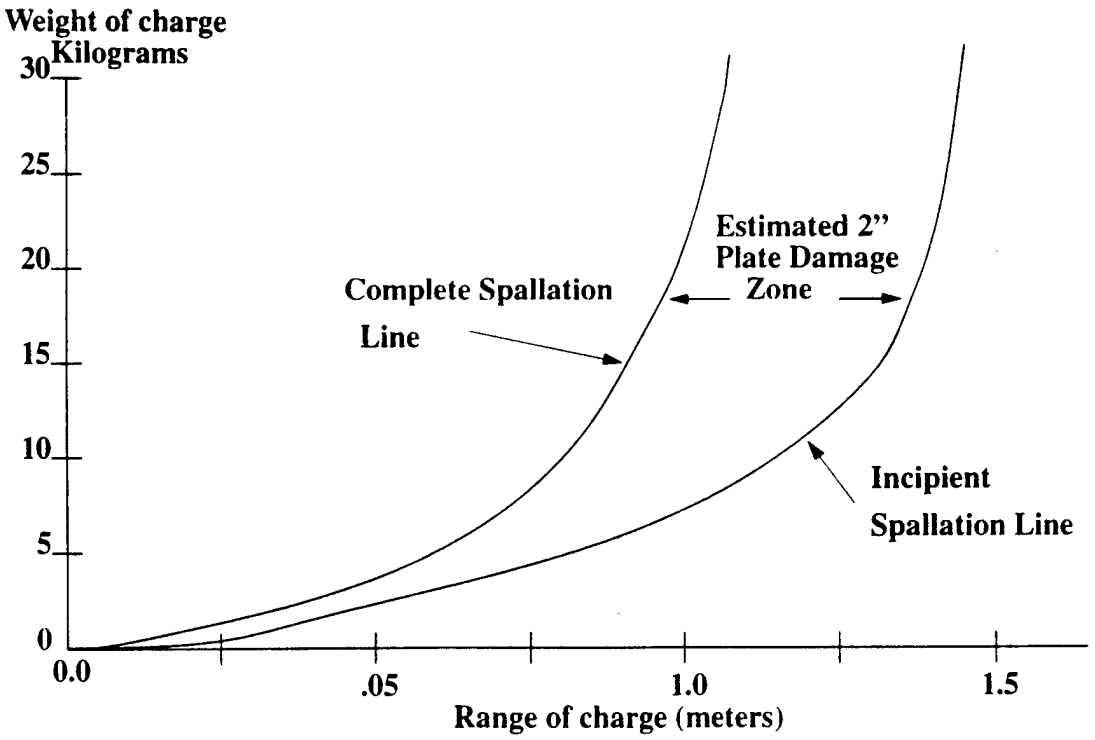

Figure 3.2a Predicted spallation (V1) damage for TNT in water and a graphite/ peek plate (2").

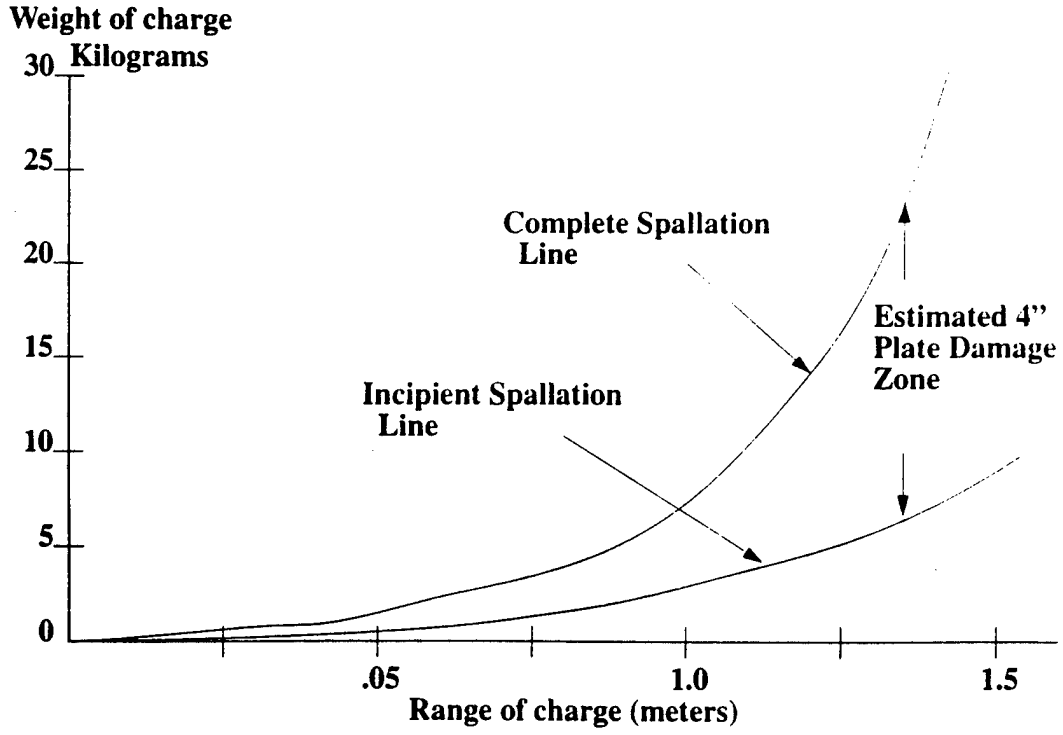

Figure 3.2b Predicted spallation (V1) damage for TNT in water and a graphite/ peek plate (4").

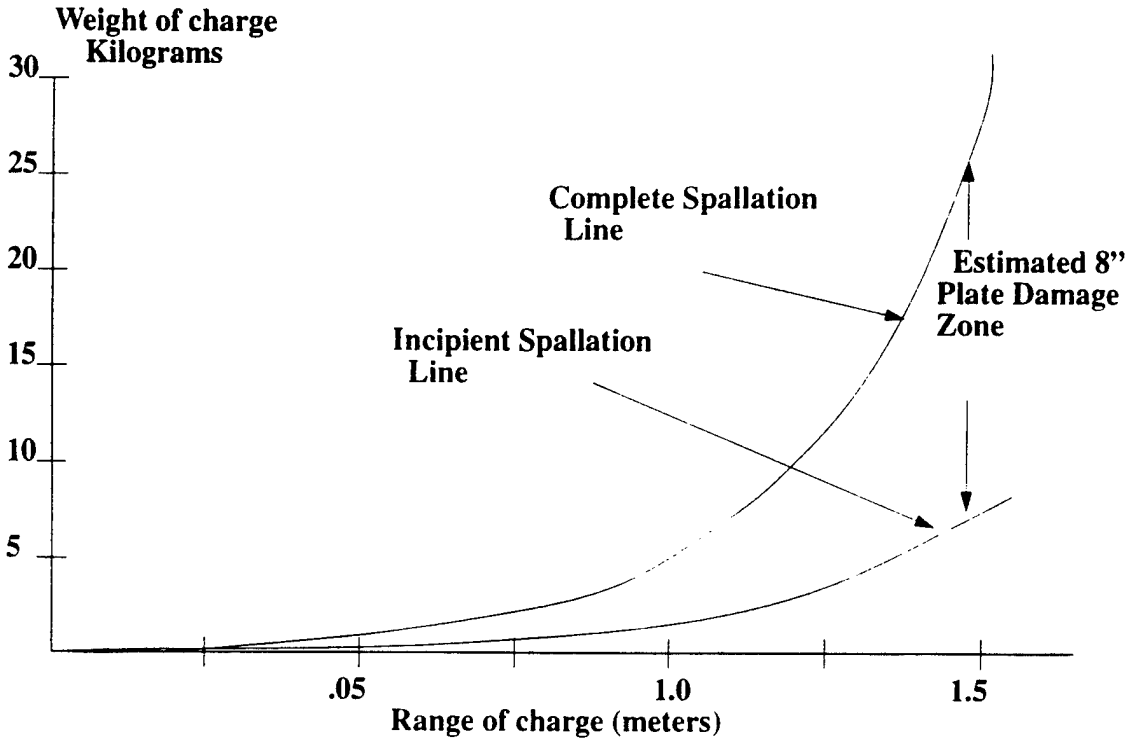

Figure 3.2c Predicted spallation (V1) damage for TNT in water and a graphite/ peek plate (8").

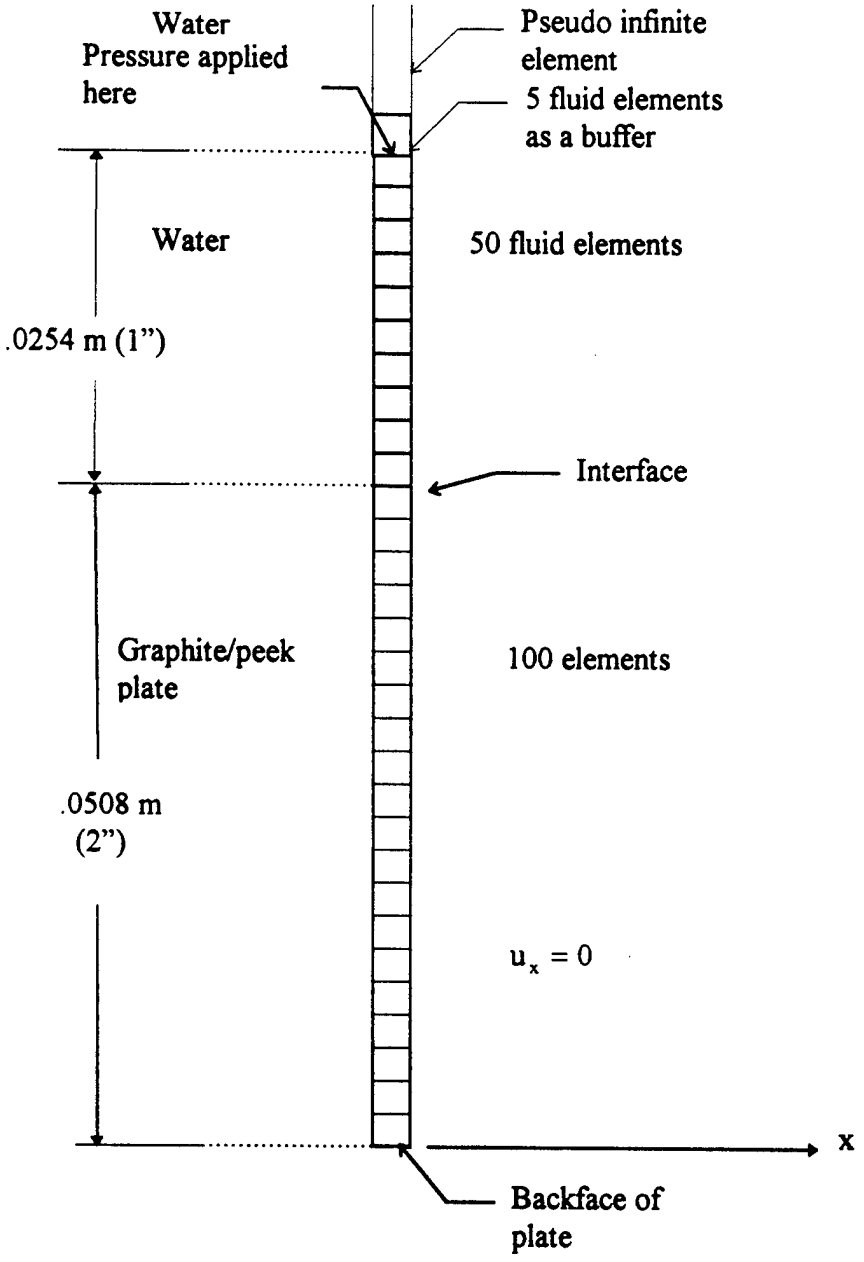

Figure 3.3 ABAQUS/EXPLICIT 2D model for 1D fluid-structure interaction.

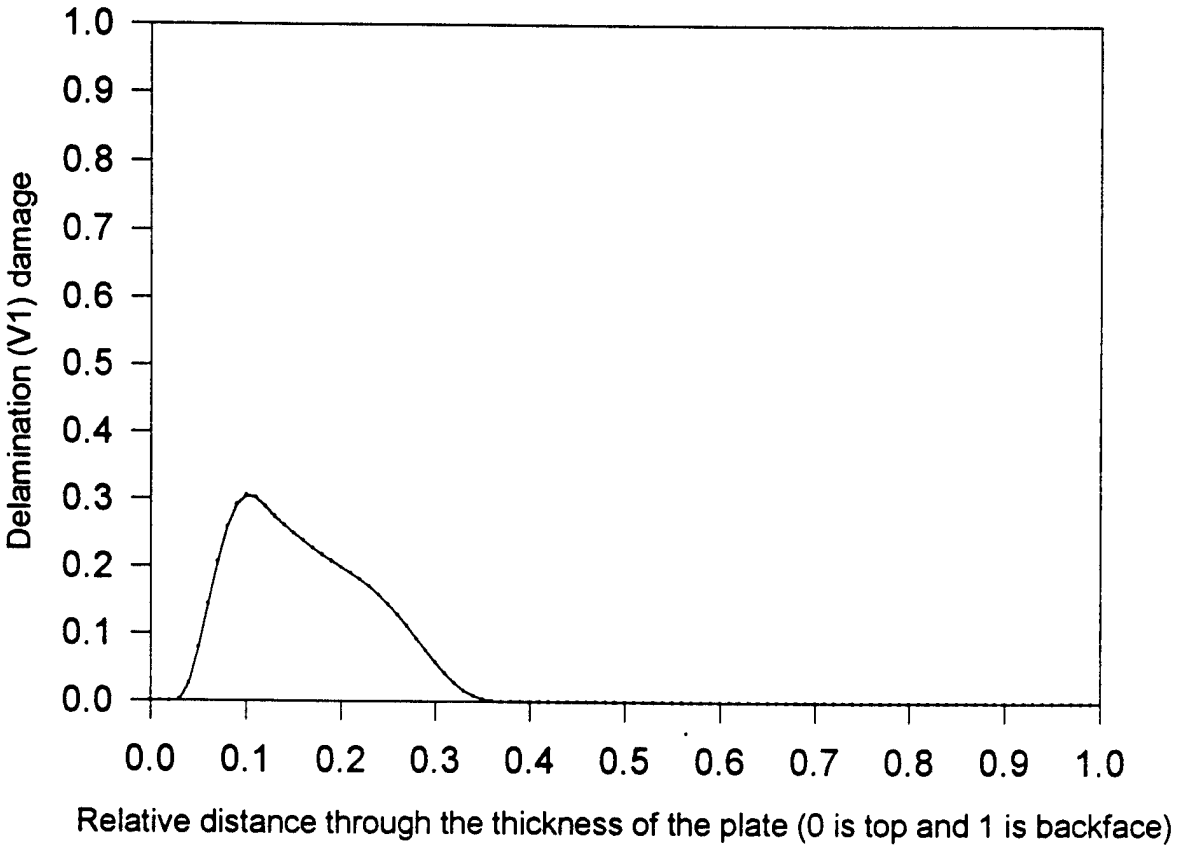

Figure 3.4 Damage results through a 2" plate from an ABAQUS/EXPLICIT fluid-structure interaction model.

4. 3D CONTINUUM DAMAGE

The development of a suitable 3D continuum damage theory for transient problems has not been an easy undertaking. A simple extension to the 2D theory [19-21] was not viable. The heterogeneity of composite structures, especially in the through thickness direction, as well as the directionality of the damage requires some sort of additional homogenization assumptions to reduce the problem to a managable state.

In [22], the Nemes and Randles [19-21] 2D continuum damage model (CDM) was extended to 3D. This section is essentially a brief summary of the 3D phenomenological theory or CDM3D that is contained in [22]. At the time of the writing of this report, a preliminary version of the CDM3D has been programmed into ABAQUS/EXPLICIT as a user written subroutine, but this capability has not yet been tested.

Essentially, the 2D continuum damage model assumes transverse isotropy in the 1-2 plane as indicated in Figure 4.1. (Note the relabeling of the 1,2, and 3 axes in Figure 4.1 from Figure 2.1.1 to allow the 3 direction to be through the thickness of the composite). Delamination damage, representing a network of matrix cracks aligned in the 1-2 plane with normals in the the 3 direction is denoted by V_3 (V_1 in [19-21]) and depicted in Figure 4.2. Inplane matrix cracks, which may traverse or lie between reinforcing fibers but not break fibers, are indicated in Figure 4.3 and referred to as V_S damage in [19-21]. In this 2D approach, damage effects were tracked and applied to the engineering moduli, shear moduli, and Poisson's ratios.

The assumption of transverse isotropy in the 2D formulation represents a reasonable approximation that allows the through thickness direction to be more easily discretized. This approximation eliminates the requirement of tracking each individual ply and the various compliances associated with them. It represents essentially a homogenization of the laminate. Note , however, a large number of elements are still required in the through thickness direction to accurately model transient through thickness effects.

In a 3D model of a laminated composite, the transverse isotropy assumption is no longer valid. Total damage which will be represented by the vector $\underline{D}$, can be expressed is the same form as (2.1) or:

$$\underline{D} = D_1 \underline{e}_1 + D_2 \underline{e}_2 + D_3 \underline{e}_3 \tag{4.1}$$

where again $\underline{e}_i$ are the unit base vectors and D_i are individual components of damage with normals aligned in the $\underline{e}_i$ direction.

A direct extension of the 2D damage model to 3D seems logical at first glance. (In the 2D theory D_1 and D_2 or V_2 and V_3 in section 2 and [19-21] are simply combined into V_S). However, a direct extension from 2D is very inefficient because it would necessitate the tracking of each individual ply and its compliances.

An alternate approach to the modeling of 3D damage is to track the damage and apply it to the stresses as is done in [32-33], as opposed to the compliances as is done in the 2D model. Solving (1.1) for D yields:

$$D = \frac{A - \bar{A}}{A} \tag{4.2}$$

D can thus be interpreted as the relative reduction in area caused by damage due to micro-cracking. For general anisotropic damage in three dimensions, the effective stress $\bar{\sigma}$ can be expressed in a tensorial form as:

$$\underline{\bar{\sigma}} = \underline{\underline{M}}(\underline{D})\underline{\sigma} \tag{4.3}$$

where $\underline{\underline{M}}$ is the material damage matrix, and $\underline{D}$ is the damage vector whose components are defined in a fashion similar to (4.2). In [32-33], the following form of $\underline{\underline{M}}$ is proposed to account for anisotropic material damage in the principal coordinate system:

$$\underline{\underline{M}} = \begin{bmatrix} \frac{1}{1-\alpha_1 D_1} & 0 & 0 & 0 & 0 & 0 \\ 0 & \frac{1}{1-\alpha_2 D_2} & 0 & 0 & 0 & 0 \\ 0 & 0 & \frac{1}{1-\alpha_3 D_3} & 0 & 0 & 0 \\ 0 & 0 & 0 & \frac{1}{[(1-\alpha_1 D_1)(1-\alpha_2 D_2)]^{**}.5} & 0 & 0 \\ 0 & 0 & 0 & 0 & \frac{1}{[(1-\alpha_1 D_1)(1-\alpha_3 D_3)]^{**}.5} & 0 \\ 0 & 0 & 0 & 0 & 0 & \frac{1}{[(1-\alpha_2 D_2)(1-\alpha_3 D_3)]^{**}.5} \end{bmatrix} \tag{4.4}$$

where, as in 2D damage theory, the fractions $0<\alpha_i<1$, I=1,2,3 have been added to prevent a complete loss of material integrity as the individual components of damage D_i go to 1.

For individual plies (4.3) and (4.4) can be easily applied, since the principal directions are in the 1-2 plane (see Figure 4.1) and perpendicular to it. Then the stress tensor $\underline{\sigma}$ can be transformed to

the global 1-2 axes. In this work, we will apply (4.3) and (4.4) to groups of plies, and assume the additional approximation that the global 1-2 axes represent the principal axes. In general for laminated composites, the 1 and 2 directions will not correspond to the principal directions. This assumption, however, can be partially rectified by adjusting the thresholds for damage to more accurately reflect the grouping of the individual plies within a single finite element.

For linear elasticity, the relationship between the stress and the strain tensors can be written as:

$$\underline{\sigma} = \underline{\underline{C}}\,\underline{\varepsilon} \tag{4.5}$$

where $\underline{\underline{C}}$ is the constitutive tensor and $\underline{\varepsilon}$ is the strain. In the case of an orthotropic lamina in which there is no coupling between the shear stresses:

$$\begin{bmatrix} \sigma_{11} \\ \sigma_{22} \\ \sigma_{33} \\ \sigma_{12} \\ \sigma_{13} \\ \sigma_{23} \end{bmatrix} = \begin{bmatrix} C_{11} & C_{12} & C_{13} & 0 & 0 & 0 \\ C_{21} & C_{22} & C_{23} & 0 & 0 & 0 \\ C_{31} & C_{32} & C_{33} & 0 & 0 & 0 \\ 0 & 0 & 0 & C_{44} & 0 & 0 \\ 0 & 0 & 0 & 0 & C_{55} & 0 \\ 0 & 0 & 0 & 0 & 0 & C_{23} \end{bmatrix} \begin{bmatrix} \varepsilon_{11} \\ \varepsilon_{22} \\ \varepsilon_{33} \\ \varepsilon_{12} \\ \varepsilon_{13} \\ \varepsilon_{23} \end{bmatrix} \tag{4.6}$$

where 1,2 and 3 are the principal axes. In terms of the engineering constants, the components of the constitutive tensor $\underline{\underline{C}}$ are:

$$\begin{aligned} C_{11} &= (1 - \nu_{23}\nu_{23}) / (E_2 E_3 \beta) \\ C_{12} &= (\nu_{12} + \nu_{32}\nu_{13}) / (E_1 E_3 \beta) = C_{21} \\ C_{13} &= (\nu_{13} + \nu_{12}\nu_{23}) / (E_1 E_2 \beta) = C_{31} \\ C_{22} &= (1 - \nu_{13}\nu_{31}) / (E_1 E_3 \beta) \\ C_{23} &= (\nu_{23} + \nu_{21}\nu_{13}) / (E_1 E_2 \beta) = C_{32} \\ C_{33} &= (1 - \nu_{12}\nu_{21}) / (E_1 E_2 \beta) \\ C_{44} &= G_{12}, \qquad C_{55} = G_{13} \qquad C_{66} = G_{23} \end{aligned} \tag{4.7}$$

and

$$\beta = (1 - \nu_{12}\nu_{21} - \nu_{23}\nu_{32} - \nu_{31}\nu_{13} - 2\nu_{21}\nu_{32}\nu_{13}) / (E_1 E_2 E_3)$$

where ν_{ij}, E_i and G_i represent the various Poisson ratios, the engineering and shear moduli. In addition, there is also the following relationship:

$$\nu_{ij} / E_i = \nu_{ji} / E_j \tag{4.8}$$

in which the summation convention has been suspended.

Equations (4.3) - (4.7) can be constructed for each individual ply. However as discussed previously, it is not our intent to track the damage in each ply but rather in groups of plies. This latter approach is much more feasible. For 3D and 2D solid finite element, explicit transient analysis, programs such as ABAQUS/EXPLICIT employ linear (interpolation) solid elements with reduced or one point integration. With this in mind, equations (4.5) - (4.8) can be applied to groups of plies and their homogenized effect into one or more elements. With a linear element due to one point integration, the stress and strain do not vary in the through thickess direction (or in the other two direction as well). Thus (4.6) for a group of N plies can be written as:

$$\underline{\sigma} = \sum_{i=1}^{N} \underline{\underline{C}}_i \underline{\varepsilon} \tag{4.9}$$

In lumping together groups of plies and orientations (a,b,c,d) for instance, we appear to be restricting the number of elements allowed in the 3 direction. In some instances over 100 elements through the thickess may be required to track the wave nature of the response and ensuing damage. If there are only 10 groups of plies with orientations of say (a,b,c,d) with this approach only 40 elements in the 3 direction could be allowed before individual plies would have to be modeled with more than one element. This approach would also be very difficult with respect to pre-processing. To overcome this defficiency, an additional approximation is introduced, which assumes each group of plies can be broken down into subgroups with exactly the same group of plies as the original group but with scaled thicknesses. Thus, if as in this case, there are 10 groups of plies with orientations of (a,b,c,d) and 100 elements through the thickness are required , is assumed that there are 100 groups of plies (a,b,c,d) with thickness 1/10 of the original layup. This latter homogenization approximation appears to be a reasonable compromise to the modeling of each individual ply, or the possibility of requiring more than one element per ply should additional elements in the 3 direction be necessary. Of course, a more drastic homogenization simplification such as assuming averaged orthotropic properties through the entire thickness can also be made with equations (4.2) - (4.7).

We now return to (4.3) and (4.4). The strain energy W of an undamped material can be expressed as:

$$W = \frac{1}{2}\underline{\sigma}^T\underline{\varepsilon} \tag{4.10}$$

Using (4.6), (4.10) becomes:

$$W = \frac{1}{2}\underline{\varepsilon}^T\underline{\underline{C}}\underline{\varepsilon} \tag{4.11}$$

in terms of the strain tensor ε or

$$W = \frac{1}{2}\underline{\sigma}^T\underline{\underline{C}}^{-1}\underline{\sigma} \tag{4.12}$$

with respect to the stress tensor. The strain energy W_D for the damaged material is of the form:

$$W_D = \frac{1}{2}\underline{\bar{\sigma}}^T\underline{\underline{C}}^{-1}\underline{\bar{\sigma}} \tag{4.13}$$

Introducing (4.3) produces:

$$W_D = \frac{1}{2}\underline{\sigma}^T(\underline{\underline{M}}^T\underline{\underline{C}}^{-1}\underline{\underline{M}})\underline{\sigma}$$

or

$$W_D = \frac{1}{2}\underline{\sigma}^T\underline{\underline{\bar{C}}}^{-1}\underline{\sigma} \tag{4.14}$$

where

$$\underline{\underline{\bar{C}}}^{-1} = \underline{\underline{M}}^T\underline{\underline{C}}^{-1}\underline{\underline{M}} \tag{4.15}$$

Inverting (4.15) produces the damaged constitutive tensor:

$$\underline{\underline{\bar{C}}} = \underline{\underline{M}}^{-1}\underline{\underline{C}}\,(\underline{\underline{M}}^T)^{-1} \tag{4.16}$$

Because of (4.4), $\underline{\underline{M}}$ is assumed to be a diagonal matrix and thus its inverse is easy to obtain.

Having postulated an approach to model 3D continuum damage, the specific details pertaining to the evolving 3D damage model are described. The intended application is for composite materials which ususally contain a great number of imperfection sites from which cracks can grow. Thus, the nucleation of new cracks is not addressed. Rather, the focus is on the growth and evolution of damage.

Recall that the damage $\underline{D}$ is assumed to be a vector with the components D_i in the 1,2 and 3 directions. As in the 2D model [19-20], the evolution of individual components of damage are assumed to be governed by a threshold in the form:

$$F_i(\underline{\sigma}, f_i(D_j)) \le 0 \quad \text{for no damage growth} \qquad (4.17)$$

$$> 0 \quad \text{for damage growth}$$

where (i,j)=1,2,3 and there is no sum on i; F_i are scalar threshold functions; $\underline{\sigma}$ is the current stress tensor; and f_i is an array of current threshold parameters which are functions of D_j, the damage component. F_i is assumed to be of the Mohr-Coulomb yield surface [28] type and to be dependent upon the scalar stress measures σ_t and τ (tension and shear) as follows:

$$F_i(\sigma_t, \tau, f) = (1 + (\frac{\tau}{f_{3i}})^2)^{1/2} - (f_{1i} - \sigma_t) / f_{2i} \qquad (4.18)$$

In (4.18), the parameters are related to specific growth threshold strengths σ_{Gi} and τ_{Gi}, and the Coulomb friction tangent φ_{Gi} as:

$$\sigma_{Gi} = f_{1i} - f_{2i}$$

$$\tau_{Gi} = f_{3i}((f_{1i} / f_{2i})^2 - 1)^{1/2} \qquad (4.19)$$

$$\varphi_{Gi} = f_{3i} / f_{2i}$$

The tension and shear growth thresholds as well as the Coulomb friction tangent in (4.19) are assumed to be functions of the damage D_i. The threshold surface (F=0) defined by (4.18) is shown in Figure 4.4 along with the various parameters. Note that in this figure d is the shortest distance from an external state (σ_t, τ) to the threshold surface.

Using (4.18) and (4.19), we further develop the details for the components of damage D_i and its evolution. For D_3 type of damage, which corresponds to delamination, the stress measures σ_{ti} and τ_i are postulated to be of the form:

$$\sigma_{t3} = \sigma_{33} \qquad (4.20)$$

$$\tau_3 = (\sigma_{31}^2 + \sigma_{32}^2)^{1/2}$$

The growth threshold stresses and the Coulomb friction tangent in (4.19) are then taken to be:

$$\sigma_{G3} = (1 - D_3^2)\sigma_{G30}$$

$$\tau_{G3} = (1 - D_3^2)\tau_{G30} \tag{4.21}$$

$$\varphi_{G3} = \varphi_{G30} + D_3^2(\varphi_{G31} - \varphi_{G30})$$

where the "0" subscript denotes the initial undamaged properties. Note that for σ_{G3} and τ_{G3} all resistance to damage is lost as D_3 goes to 1; and the Coulomb friction tangent φ_{G1} can vary linearly with D_3^2 as the damages progresses.

From (4.18) and (4.19), the variables f_{23}, f_{13} and f_{33} are:

$$f_{23} = \frac{1}{2}\left(\frac{\tau_{G3}^2}{\varphi_{G1}^2\sigma_{G3}} - \sigma_{G3}\right)$$

$$f_{13} = \sigma_{G3} + f_{23} \tag{4.22}$$

$$f_{33} = f_2\varphi_{G3}$$

To complete the continuum damage formulation for D_3 damage, evolution equations are required. From [19-21], the following relationship is postulated for D_3 (delamination) damage:

$$\frac{dD_3}{dt} = F_3(d_3, D_3) \tag{4.23}$$

where d_3 is the shortest distance in the σ_{t3}, τ_3 stress space - see Figure 4.4 for the threshold surface $F_3 = 0$. For $d_3 = 0$, $F_3 = 0$ and $\frac{dD_3}{dt} = 0$ for all stress points interior or on the threshold surface. The specific form of (4.23) employed for the 3D theory is similar to (2.9a) with D_3 replacing V_1 and the subscript 3 replacing 1 or:

$$\frac{dD_3}{dt} = (d_3 / \sigma_{G30})^{n_3} / (\eta_3(1 - D_3^2)) \tag{4.24}$$

Next we consider D_1 and D_2 type of damage, which relate to matrix cracking. The discussion will focus on D_1, but D_2 type of damage will be assumed to be of the same form. For D_1 type of damage, the stress measures σ_{t1} and τ_1 required for (4.18) and (4.19) are postulated to be of the form:

$$\sigma_{t1} = \sigma_{11} \tag{4.25}$$

$$\tau_1 = (\sigma_{12}^2 + \sigma_{13}^2)^{1/2}$$

Equation (4.25) are used in conjunction with (4.18) and (4.19). The form of the growth threshold stresses is not of the same form as the D_3 damage, which is given by (4.20). D_1 (and also D_2) damage consist of an ever denser network of cracks which tend to saturate. There is not acceleration to a castrophic failure as in the case of D_3 damage which represents delamination. Saturation can be forced through the growth thresholds as done in [19-20] or:

$$\sigma_{G1} = \sigma_{G10} / (1 - D_1^2) \tag{4.26}$$

$$\tau_{G1} = \tau_{G10} / (1 - D_1^2)$$

while the Coulomb friction tangent is taken to be

$$\varphi_{G1} = \varphi_{G10} + D_1^2(\varphi_{G11} - \varphi_{G10}) \tag{4.27}$$

In (4.26), it is seen that as D_1 goes to 1 damage becomes more difficult since the growth thresholds σ_{G1} and τ_{G1} greatly increase.

For D_1 (and D_2) damage, the final ingredient required is the specific form of the rate evolution equation described by (4.23). Since there is no acceleration to catastrophic failure, a form similar to (2.9b) for V_s damage in the 2d theory is employed:

$$\frac{dD_1}{dt} = (d_1 / \sigma_{G10})^{n_1} / \eta_1 \tag{4.28}$$

where as in (2.9b), η_1 is a time constant, d_1 is normalized with the virgin growth threshold stress σ_{G10}, and n_1 is a positive term for the dimensionless stress distance.

Another mode of continuum damage is the breakage of the reinforcing fibers. To account for this effect, a simple maximum strain criteria is used in the 3D model. The D_1, D_2 and D_3 forms of damage cause softening of the composite response, and thus directly influence this maximum strain criteria.

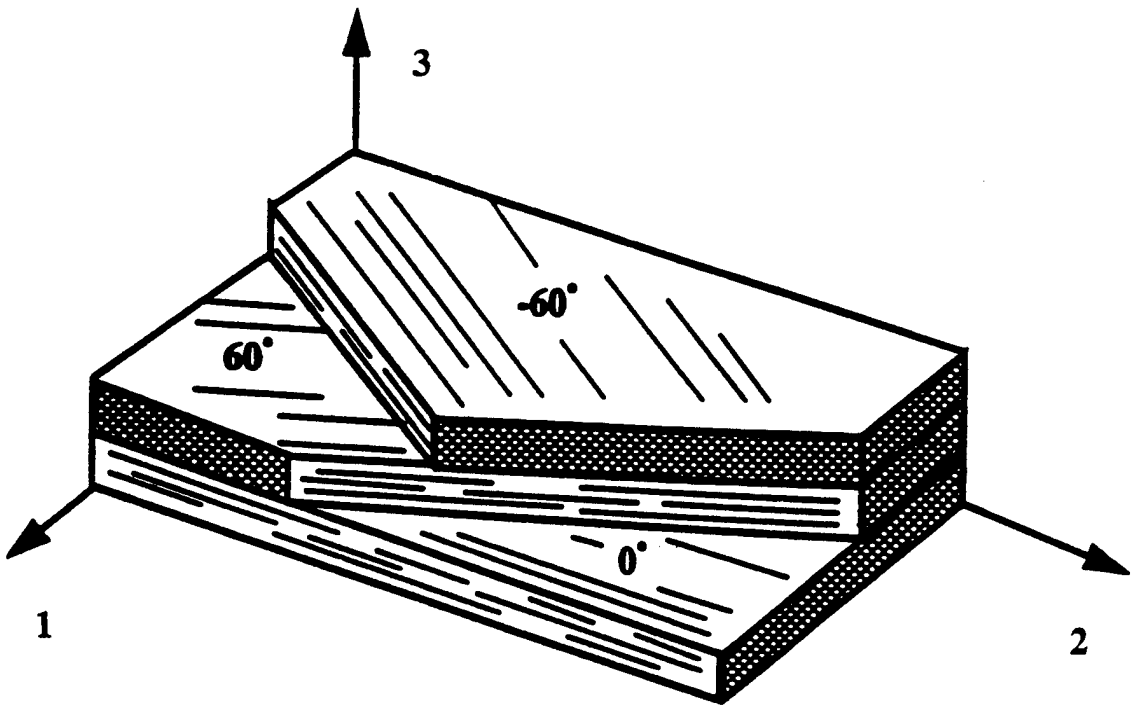

FIGURE 4.1. Portion of a 0 deg, + and - 60 deg ply layup.

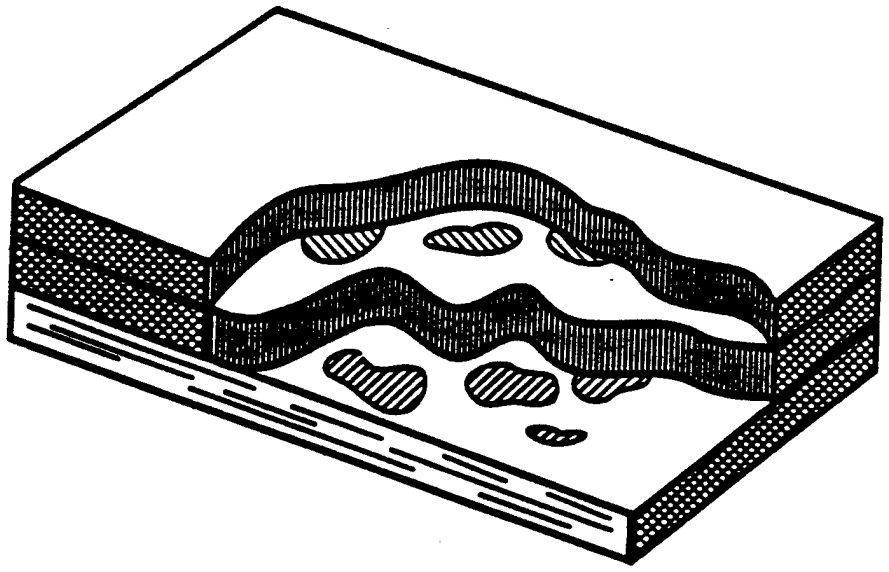

FIGURE 4.2 V_3 delamination damage.

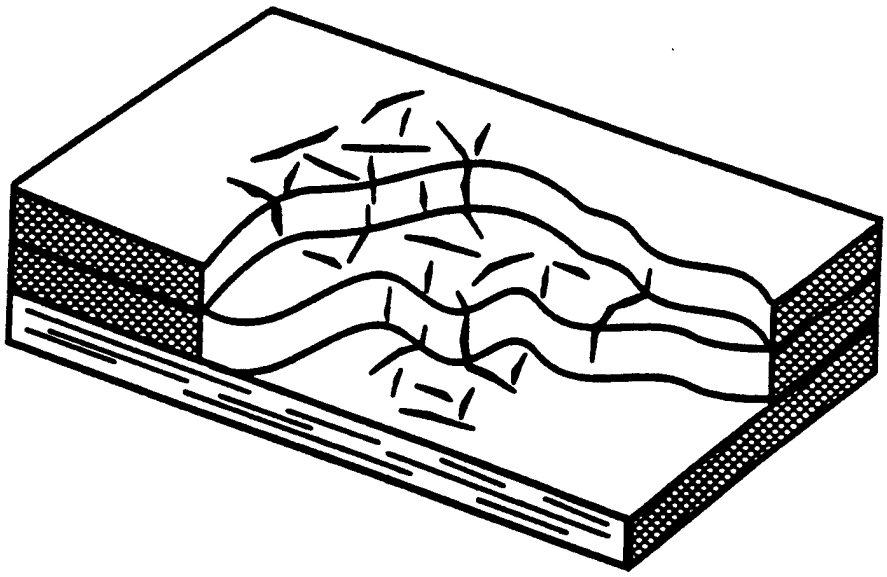

FIGURE 4.3 V_S inplane matrix damage.

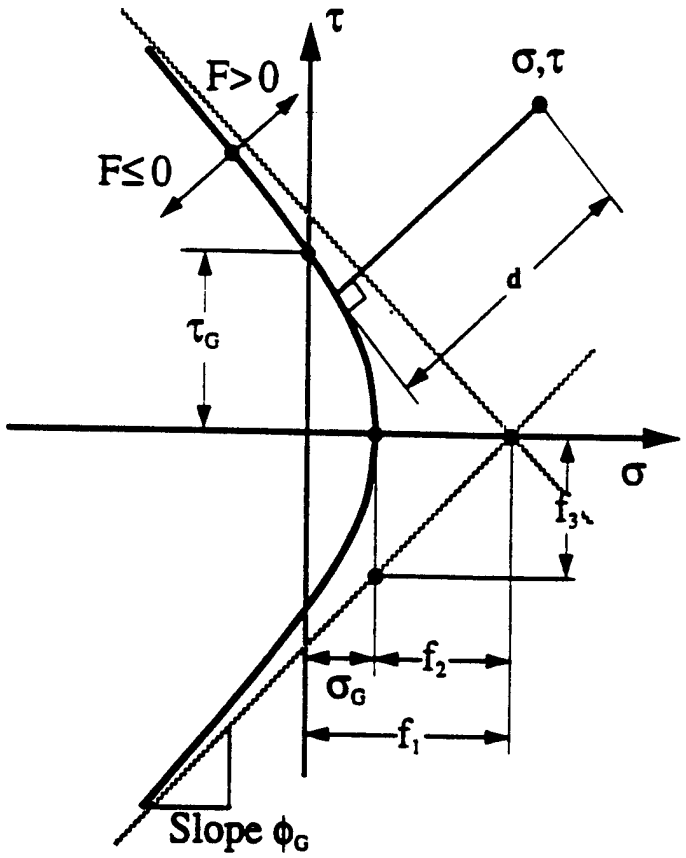

FIGURE 4.4 Threshold surface for the onset of damage.

5. SUMMARY AND CONCLUSIONS

In this report, we have discussed in the Introduction some of the difficulties associated with the modeling of the shock response and damage in marine composites. The existing technical barriers are indeed formidable but some progress has been made. Several key areas that must be addressed are: dispersion and viscoelasticity in the composite structure; homogenization assumptions; through thickness modeling and damage; and dynamic versus static properties and behavior.

In sections 2 - 5, evolving continuum damage models based primarily on the work of Nemes and Randles [19-21] have been discussed with application to 1D and 2D impact and underwater shock problems. This approach, which has been extended into 3D in [22], is phenomenological in nature requiring the determining of several empirical constants for specific composite structures. Comparisons to experimental data in [23] are good. 1D parametric studies are discussed in sections 3.1 and 3.2 for underwater shock loading environments.

In general, the phenomenological approach taken here at NRL toward the modeling of the shock response and damage in composites is of utility but is of course limited. The first author likens this situation to turbulence modeling in fluid dynamics [34-35]. No general purpose turbulence theory exists. The current turbulence models are applicable to specific flow situations and usually require some emphircal constants to be used to obtain accurate simulations. The statistical nature of turbulence is addressed using time averaging techniques and generating continuum equations containing fluctuations.

As with turbulence, the material properties as well as the shock response and evolving damage in composite structures have a non-deterministic, statistical nature that is difficult to adequately address with continuum mechanics analysis methods. The continuum assumption eventually either breaks down or must be modified as one goes from the macro to meso to micro scales. The interaction of these time scales is difficult to incorporate into a macro finite element model that is robust and accurate for a wide variety of materials and structures.

6. ACKNOWLEDGEMENT

This work was supported in part by a grant of HPC computer time from the DoD HPC Shared Resource Center at NRL on a CRAY-EL.

7. REFERENCES`

1) A. P. Mouritz, The Effect of Underwater Explosion Shock Loading on the Fatique Behavior of GRP Laminates, Composites, Vol. 26, Number 1, pp. 3-9, 1995.

2) E. A. Rasmussen and J. R. Carlberg, Shock Response of Ring Stiffened Glass/Epoxy Composite Cylinder RC-3, David Taylor Research Center, Report DTRC-SSPD-91-172-75, April 1991.

3) E. A. Rasmussen, Development of a Thick Section Composite Structural Element Test Method to Simulate Underwater Shock Response, Naval Surface Warfare Center, Carderock Division, Report SSPD-93-172-26, Dec. 1992.

4) J. Lemaitre and J. L. Chaboche, Mechanics of Solid Materials, Cambridge University Press, 1990.

5) G. A. Maugin, The Thermomechanics of Plasticity and Fracture, Chaper 10: Coupling Between Plasticity and Damage, Cambridge University Press, 1992.

6) J. Lemaitre, A Course on Damage Mechanics, Springer-Verlag, 1992.

7) J. W. Ju, D. Krajcinovic and H. L. Shreyer editors, Damage Mechanics in Engineering Materials, ASME, AMD-Vol 109, 1990.

8) J. W. Ju editor, Recent Advances in Damge Mechanics and Plasticity, ASME, AMD-Vol 132, 1992.

9) J. W. Ju and K. C. Valanis, Damage Mechanics and Localization, ASME, AMD-Vol 142,1992.

10) D. H. Allen and D. C. Lagoudas editors, Damage Mechanics in Composites, ASME, AMD-Vol. 150, 1992.

11) D. R. Curran, L. Seamen and D. A. Shockey, Dynamic Failure of Solids, Physics Reports, Vol. 147, pp. 253-388, 1987.

12) L. Davison and A. L. Stevens, Thermomechanical Constitution of Spalling Elastic Bodies, Journal of Applied Physics, Vol. 44, No. 2, pp. 668-674, 1972.

13) D. Krajcinovic, Damage Mechanics, Mechanics of Materials, Vol. 8, pp. 117-197, 1989.

14) R. Talreja, A Continuum Mechanics Characterization of Damage in Composite Materials, Proceedings Royal Society, Vol. A399, pp. 195-216, 1985.

15) L. M. Kachanov, On the Creep Fracture Time, Izv. Akad. Nauk U.S.S.R. Otd. Tekh. 8, pp. 26-31, 1958.

16) Y. N. Rabotnov, Creep Problems in Structural Members, North Holland, 1969.

17) C. T. Dyka, R. P. Ingel and L. D. Flippen, A New Approach to Dynamic Condensation for FEM, to appear in Computers and Structures.

18) P. W. Mast, G. E. Nash, J. Michopoulos, R. W. Thomas, R. Badaliance and I. Wolock, Experimental Determination of Dissipated Energy Density as a Measure of Strain-Induced Damage in Composites, NRL Report, NRL/FR/6383-9369, April 17, 1992.

19) J. A. Nemes and P. W. Randles, Modelling the Response of Thick Composite Materials Due to Axisymmetric Shock Loading, NRL Memorandom Report 6856, August 5, 1991.

20) P. W. Randles and J. A. Nemes, A Continuum Damage Model for Thick Composite Materials Subjected to High-rate Dynamic Loading, Mechanics of Materials, Vol. 13, No. 1, pp. 1-13, 1992.

21) J. A. Nemes and P. W. Randles, Constitutive Modeling of High Strain-rate Deformation and Spall Fracture of Graphite/Peek Composites, Mechanics of Materials 19, pp. 1-14, 1994.

22) C. T. Dyka and P. W. Randles, Progress in the Modeling of the Shock Response and Mitigation of Thick Composite Shells, NRL Memorandom Report, NRL/MR/6386-93-7369, July 22, 1993.

23) E. A. Smith, Shock Response of Two Thick Composite GR-EP and GR-PEEK, Report TR-91/02, Ktech Corporation, Albuquerque, NM, August 1991.

24) J. A. Nemes, A Viscoplastic Description of High Strain-Rate Deformation, Material Damage, and Spall Fracture, Ph.D. Dissertation, George Washington University, 1989.

25) J. Eftis, J. A. Nemes and P. W. Randles, Viscoplastic Analysis of Plate-Impact Spallation, International Journal of Plasticity, Vol. 7, pp. 15-39,1991.

26) J. A. Nemes and J. Eftis, Pressure-Shear Waves and Spall Fracture Describe by a Viscoplastic Damage Constitutive Model, International Journal of Plasticity, Vol. 8, 1992.

27) P. Perzyna, Internal State Variable Description of Dynamic Fracture of Ductile Solids, International Journal of Solids and Structures, 22(7), pp. 797-818, 1986.

28) C. S. Desai and H. J. Siriwardane, Constitutive Laws for Engineering Materials with Emphasis on Geologic Materials, Prentice-Hall, 1984.

29) M. E. Kipp and R. J. Lawrence, WONDY5- A One Dimensional Finite Difference Wave Propagation Code, SANDIA Report 81-0930.UC-32, June 1982.

30) K. M. Wu, Preliminary Modeling of Compressive Shock and Spallation in Thick Composite Materials, NRL Memorandum Report 6684, July 1990.

31) R. J. Dunst, W. Lauder, and K. Weisenborn, Destructive Evaluation of Thick Composite Samples, Report 1670, Touchstone Research Laboratory, Ltd., Triadelphia, WV, Dec. 1993.

32) C. L. Chow and J. Wang, An Anisotropic Theory of Elasticity for Continuum Damage Mechanics, International Journal of Fracture 33, pp. 3-16, 1987.

33) J. Wang and C. L. Chow, A Non-proportional Loading Finite Element Analysis of Continuum Damage Mechanics for Ductile Fracture, Inter. Jour. Num. Meth. Engin., Vol. 29, pp. 197-209, 1990.

34) M. T. Landahl and E. Mollo-Christensen, Turblence and Random Processes in Fluid Mechanics, Cambridge University Press, 1986.

35) J. O. Hinze, Turbulence, second edition, McGraw-Hill, 1975.